Uncertainty and sensitivity analysis of the basic reproduction number of diphtheria: A case study of Rohingya refugee camp in Bangladesh, November-December 2017

Ryota Matsuyama [1,2], **Andrei R Akhmetzhanov** [1,2], **Akira Endo** [1,3], **Hyojung Lee** [1,2], **Takayuki Yamaguchi** [1,2], **Shinya Tsuzuki** [1,2], **Hiroshi Nishiura** [Corresp. 1,2]

[1] Graduate School of Medicine, Hokkaido University, Sapporo, Japan

[2] Japan Science and Technology Agency, Core Research for Evolutional Science and Technology, Saitama, Japan

[3] London School of Hygiene & Tropical Medicine, University of London, London, United Kingdom

Corresponding Author: Hiroshi Nishiura
Email address: nishiurah@gmail.com

Background. A Rohingya refugee camp in Cox's Bazar, Bangladesh experienced a large-scale diphtheria epidemic in 2017. The background information of previously immune fraction among refugees cannot be explicitly estimated, and thus, we conducted an uncertainty analysis of the basic reproduction number, R0. **Methods.** A renewal process model was devised to estimate the R0 and ascertainment rate of cases, and loss of susceptible individuals was modeled as one minus the sum of initially immune fraction and the fraction naturally infected during the epidemic. To account for the uncertainty of initially immune fraction, we employed a Latin Hypercube sampling (LHS) method. **Results.** R0 ranged from 4.7 to 14.8 with the median estimate at 7.2. R0 was positively correlated with ascertainment rates. Sensitivity analysis indicated that R0 would become smaller with greater variance of the generation time. **Discussion.** Estimated R0 was broadly consistent with published estimate from endemic data, indicating that the vaccination coverage of 86% has to be satisfied to prevent the epidemic by means of mass vaccination. LHS was particularly useful in the setting of refugee camp in which the background health status is poorly quantified.

1 **Uncertainty and sensitivity analysis of the basic reproduction**

2 **number of diphtheria: A case study of Rohingya refugee**

3 **camp in Bangladesh, November-December 2017**

5 Ryota Matsuyama[1,2], Andrei R. Akhmetzhanov[1,2], Akira Endo[1,3], Hyojung Lee[1,2], Takayuki

6 Yamaguchi[1,2], Shinya Tsuzuki[1,2], Hiroshi Nishiura[1,2§]

8 [1.] Graduate School of Medicine, Hokkaido University, Sapporo, Japan

9 [2.] CREST, Japan Science and Technology Agency, Saitama, Japan

10 [3.] London School of Hygiene and Tropical Medicine, London, United Kingdom

12 Corresponding Author:

13 Hiroshi Nishiura

14 Graduate School of Medicine, Hokkaido University, Sapporo, Japan

15 Kita 15 Jo Nishi 7 Chome, Kita-ku, Sapporo-shi, Hokkaido 060-8638, Japan

16 Email address: nishiurah@med.hokudai.ac.jp

18 **Abstract**

19 **Background**

20 A Rohingya refugee camp in Cox's Bazar, Bangladesh experienced a large-scale diphtheria

21 epidemic in 2017. The background information of previously immune fraction among refugees

22 cannot be explicitly estimated, and thus, we conducted an uncertainty analysis of the basic

23 reproduction number, R_0.

24 **Methods**

25 A renewal process model was devised to estimate the R_0 and ascertainment rate of cases, and loss

26 of susceptible individuals was modeled as one minus the sum of initially immune fraction and

27 the fraction naturally infected during the epidemic. To account for the uncertainty of initially

28 immune fraction, we employed a Latin Hypercube sampling (LHS) method.

29 **Results**

30 R_0 ranged from 4.7 to 14.8 with the median estimate at 7.2. R_0 was positively correlated with

31 ascertainment rates. Sensitivity analysis indicated that R_0 would become smaller with greater

32 variance of the generation time.

33 **Discussion**

34 Estimated R_0 was broadly consistent with published estimate from endemic data, indicating that

35 the vaccination coverage of 86% has to be satisfied to prevent the epidemic by means of mass

36 vaccination. LHS was particularly useful in the setting of refugee camp in which the background

37 health status is poorly quantified.

38

Introduction

Diphtheria, a bacterial disease caused by *Corynebacterium diphtheriae*, is a vaccine-preventable disease. Symptomatic patients initially complain sore throat and fever. Additionally, a grey or white patch causes the "croup", blocking the airway and causing a barking cough. Due to widespread use of Diphtheria-Tetanus-Pertussis (DTP) vaccine globally, the incidence has steadily declined over time, and thus, diphtheria is commonly perceived as almost a disease of pre-vaccination era. Nevertheless, sporadic cases and even epidemics of the disease have been yet reported especially in politically unstable areas, and many cases have been considered as arising from susceptible pockets of the vulnerable population (Rusmil et al., 2015; Hosseinpoor et al., 2016; Sangal et al., 2017).

In 2017, multiple diphtheria outbreaks were reported in refugee camps, including those in Yemen and Bangladesh (World Health Organization (WHO), 2017a). Of these, a Rohingya refugee camp in Bangladesh, which is temporarily located in Cox's Bazar, experienced a large-scale diphtheria epidemic. As of 26 December 2017, the cumulative number of 2,526 cases and 27 deaths were reported (WHO, 2017a). To interrupt chains of transmission, emergency vaccination has been conducted among children since 12 December 2017, achieving the overall coverage greater than 90% by the end of 2017 (WHO, 2018). Due to vaccination effort and other countermeasures, including contact tracing and hospital admission of cases, the epidemic has been brought under control, with incidence beginning to decline by the end of December 2017 (WHO, 2017a).

Considering that diphtheria has become a rare disease in industrialized countries, epidemiological information on model parameters that govern the transmission dynamics has become very limited, and thus, it is valuable to assess how transmissible diphtheria would be

62 through the analysis of the recent outbreak data. The basic reproduction number, R_0, is

63 interpreted as the average number of secondary cases that are produced by a single primary case

64 in a fully susceptible population, acting as the critical measure of the transmissibility. To date, an

65 explicit epidemiological estimate of R_0 for diphtheria has been reported only by Anderson and

66 May (1982): using a static modeling approach to age-dependent incidence data with an

67 assumption of the endemic equilibrium, R_0 was estimated as 6.6 in Pennsylvania, 1910s and 6.4

68 in Virginia and New York from 1934-47. Subsequently, a few additional modeling studies of

69 diphtheria took place (Kolibo, 2001; Sornbundit, 2017; Torrea, 2017), but none of these offered

70 an empirical estimate of R_0.

71   Here we analyze the epidemiological dataset of diphtheria in Rohingya refugee camp,

72 2017, aiming to estimate R_0 in this particular epidemic setting. Given that the epidemic occurred

73 among refugees, we explicitly account for uncertainties associated with unknown background

74 information, including the fraction of previously immune individuals and ascertainment rate of

75 cases.

Materials & Methods

Epidemiological data

78 The latest epidemic curve was extracted from the report of the World Health Organization

79 (WHO) Regional Office for South East Asia (SEARO) (WHO, 2017a). Figure 1 shows the latest

80 available epidemic curve. As of 26 December 2017 (the latest date of observation), a total of

81 2,526 cases have been reported. Cases consist of (i) confirmed cases: cases reported as positive

82 for *C. diphtheria*e by multiplex assay, (ii) probable cases: cases with upper respiratory tract

83 illness with laryngitis or nasopharyngitis or tonsillitis AND sore throat or difficulty swallowing

84   and an adherent membrane (pseudomembrane) OR gross cervical lymphadenopathy, and (iii)

85   suspected cases: any case with a clinical suspicion of diphtheria, including cases that are

86   unclassified due to missing values (WHO, 2017b). Prior to 11 December 2017, cases satisfied

87   only the condition of suspected cases. The definition was improved on and after 12 December

88   (WHO, 2017c), enforcing to count mainly probable cases, while not restricting the reporting of

89   suspected cases. For this reason, cases reported by 11 December are considered to have been

90   perhaps over-ascertained compared with cases that were reported later under improved case

91   definition. Mass child vaccination started on 12 December, and according to the administrative

92   coverage, greater than 90% vaccination coverage was achieved by 30 December (WHO, 2018).

93   Vaccine-induced immunity requires at least 7-14 days to become effective, and moreover, the

94   reporting delay was assumed to be about 4 days (based on additional analyses; Results not

95   shown). For these reasons, the dataset from 23-26 December was discarded as the number of

96   cases may be influenced by emergency vaccination and also biased by the reporting delay.

97   **Modeling methods**

98   To formulate the epidemiological model, here we mathematically capture the epidemiological

99   process of secondary transmission using R_0 and the serial interval, i.e., the time from illness

100 onset in the primary case to illness onset in the secondary case. We assume that secondary

101 transmission does not take place before illness onset. According to a classical study by Stocks

102 (1930) in the United Kingdom (UK), the time interval from first to second diphtheria cases in the

103 household revealed a bimodal shape. Following Klinkenberg and Nishiura (2011), the first peak

104 corresponds to an independent infection in the community and the second peak reflects within-

105 household transmission. As one of peak time-lags in the observed time interval was observed on

106 day 8, we assumed that the mean serial interval was 8 days, and we imposed an assumption that

107   the coefficient of variation (CV) of the serial interval distribution was 50%, and later varied it

108   from 25% to 75% as part of the sensitivity analysis.

109   To capture the epidemiological phenomena of reproduction, it is very well known that the

110   renewal process can capture the serial stochastic dependence structure (Nishiura, 2010). Let i_t be

111   the number of new cases on day t. g_τ represents the distribution of the serial interval. To describe

112   the time-dependent incidence i_t on day t, we have

113
$$i_t = R_0 s_t \sum_{\tau=1}^{t-1} i_{t-\tau} g_\tau \,,$$
(1)

114   where s_t represents the fraction of susceptible individuals on day t. The renewal process of this

115   type is not original to the present study and has been applied to other settings including real-time

116   epidemic modelling studies (Asai & Nishiura, 2017; Dinh et al., 2016; Ejima & Nishiura, 2018;

117   Endo & Nishiura, 2015; Nishiura et al., 2010; Nishiura et al., 2016; Tsuzuki et al., 2017). It

118   should be noted that the incidence i_t includes both symptomatic and asymptomatic cases. Let c_t

119   be the reported number of cases on calendar day t. Supposing that only the fraction α_t among the

120   total number of infections are diagnosed and reported, c_t satisfies

121
$$i_t = \frac{c_t}{\alpha_t} \,,$$
(2)

122   where α_t is modeled as a function of t. Because the case definition was improved from 12

123   December 2017 onward, the ascertainment rate likely varied around that time. Namely, we set α_t

124    $=a_1$ for time by 11 December and a_2 on 12 December and later. We assumed that only the

125   ascertainment rate changed as a function of time, and also that R_0 and depletion of susceptible

126   individuals were unaffected by time.

127   We model the fraction susceptible s_t on day t in the following way. Let v represent the

128   previously immunized fraction so that only fraction $(1-v)$ of the population is susceptible at the

129   beginning of the epidemic. In addition to the previously immune fraction, s_t decreases when

130   natural infection takes place. Suppose that the total population size was N, s_t is written as

131
$$s_t = 1 - v - \frac{\sum_{y=1}^{t-1} \frac{c_y}{\alpha_y}}{N}.$$
(3)

132   We assume that N is equal to the population size of epidemic area within Rohingya refugee camp

133   as 579,384 persons (Banerji & Ahmed, 2017). Accordingly, the renewal equation is written as

134
$$E(c_t; R_0, v, a_1, a_2) = \alpha_t R_0 \left(1 - v - \frac{\sum_{y=1}^{t-1} \frac{c_y}{\alpha_y}}{N} \right) \sum_{\tau=1}^{t-1} \frac{c_{t-\tau}}{\alpha_{t-\tau}} g_\tau$$
(4)

135   where τ in the right-hand side indicates the time since infection (or the so-called "infection-age").

136   We assume that c_t follows a Poisson distribution. The likelihood to estimate θ consisting of the

137   parameters R_0, v and α_t is derived as

138
$$L(\theta; \mathbf{c_T}) = \prod_{t=1}^{T} \left(\frac{E(c_t)^{c_t} \exp(-E(c_t))}{c_t!} \right),$$
(5)

139   where T is the latest time of observation (i.e., 22 December in our case study) and $\mathbf{c_T} = (c_1, c_2, \ldots,$

140     $c_T)$.

141   **Uncertainty and sensitivity analyses**

142   While we specified unknown parameters as R_0, v and α_t, it is expected that R_0 is correlated with

143   initially immune fraction v and also α_t. Thus, it is vital to quantify R_0 while accounting for the

144   uncertainty of other model parameters. In the present study, v was most uncertain and thus

145   subject to uncertainty analysis, while α_t was estimated as a step function governed by two

146   parameters, a_1 and a_2. Uncertainty in parameter values can be addressed by randomly sampling

147   the uncertain parameter value from probability distributions (Gilbert et al., 2014). Here we use

148   the Latin Hypercube sampling (LHS) method (Sanchez & Blower, 1997) in which a symmetric

149   triangular distribution of v was assumed to be in the range from 0.0 to 0.7; the health survey of

150   Rohingya population indicated that overall 30.8% of children had received no vaccinations

151   (Guzek et al, 2017), and the remaining 69.2% receives at least a single immunization, which is

152   not necessarily against diphtheria but against a specific disease. We restrict our interest to

153   diphtheria, and thus, the vaccination coverage against diphtheria should be lower than that of

154   "any" vaccine. Thus, we expect that the actual coverage is nearby the mid-point of the range

155   from 0.0 to 0.7. In addition, we examined the sensitivity of R_0 to variations in the length of the

156   serial interval.

157   **Ethical considerations**

158   The present study analyzed data that is publicly available. As such, the datasets used in our study

159   were de-identified and fully anonymized in advance, and the analysis of publicly available data

160   without identity information does not require ethical approval.

161   # Results

162   Figure 2 shows univariate distributions of estimated parameters R_0 and α_t based on Latin

163   hypercube sampling (n=1000) of parameter v from 0 to 0.70 with the peak at 0.35. a_1 reflects

164   ascertainment by 11 December 2017, while a_2 shows the same on and after 12 December. R_0

165   took the minimum and maximum estimates at 4.7 and 14.8, respectively, with the median

166   estimate at 7.2. The distribution was skewed to the right with the mode at 6.7. Excluding lower

167   and upper tails, 950 samples (95%) of R_0 (or what it can be assumed as the 95% tolerance

168   intervals) were in the range of 5.0 to 12.3. Distributions of a_1 and a_2 were also right skewed. a_1

169   ranged from 0.007 to 0.021 with the median 0.010, while α_2 ranged from 0.003 to 0.011 with the

170   median 0.005. Lower and upper 95% tolerance intervals of a_1 and a_2 were (0.007, 0.017) and

171   (0.004, 0.009), respectively. A decline of α_t was observed, because the incidence was supposed

172   to have grown more during the early phase (i.e. by 11 December) given the estimated

173   epidemiological parameters. In practical sense, the timing coincided with the involvement of

174   contact tracing practice enforced by the Médecins Sans Frontières.

175   Figure 3 shows the distributions of two estimated parameters in two dimensional spaces

176   and also the comparison between observed and predicted epidemic curve. As can be expected

177   from equation (4), R_0 and v were positively correlated given an epidemic curve. Specifically, as v

178   increases R_0 must also increase to achieve an identical epidemic curve. Similarly, R_0 was

179   positively correlated with ascertainment rates, a_1 and a_2. While the ascertainment might have

180   been lowered due to the stricter case definition, the small estimate of a_2 can also indicate that a

181   substantial fraction of undiagnosed individuals existed and the susceptible fraction was then

182   gradually depleted in the population. The observed and predicted epidemic curves are compared

183   in the right lower panel of Figure 3. While the model is kept simple with four unknown

184   parameters, the predicted epidemic curve overall captured the observed pattern.

185   Sensitivity of R_0 to the variation in the serial interval is shown in Figure 4. We varied the

186   CV of the serial interval distribution from 25% to 75%. When the CV was 25%, the median and

187   mode of R_0 from Latin hypercube sampling were 9.4 and 8.2, respectively. When the CV was

188   75%, the median and mode of R_0 were estimated to be 5.7 and 5.2, respectively. That is, as the

189   variance increases, the estimate of R_0 decreases. However, the variation in R_0 induced by the CV

190   was smaller than the uncertainty associated with the initially immune fraction.

191

Discussion

193   The present study estimated R_0 of diphtheria in the Rohingya refugee camp, explicitly accounting

194   for case ascertainment and previously immune fraction. Since previously immune fraction v of

195   the refugee population was not precisely known, uncertainty analysis of R_0 was conducted with

196   an input parameter assumption for v employing the Latin Hypercube sampling method. R_0 ranged

197   from 4.7 to 14.8 with the median estimate at 7.2. To our knowledge, the present study is the first

198   to statistically estimate R_0 of diphtheria from epidemic data. For the statistical estimation of R_0,

199   the renewal process model was employed, which has an advantage to handle the right-censored

200   data during the course of an epidemic, compared with other available methods for completely

201   observed data, e.g., Nishiura (2010).

202   Estimated median R_0 was broadly consistent with the value ranging from 6 to 7 as

203   indicated by Anderson and May (1982) based on a static model for endemic data that uses the

204   age-dependent incidence in the UK. We have shown that the frequently quoted estimate agrees

205   well with dynamically estimated R_0 from the refugee camp in the present day. Assuming $R_0=7$, to

206   control diphtheria by means of mass vaccination, the coverage greater than 86% must be

207   satisfied. Since our study focused on uncertainty and sensitivity analyses, the exact estimate of

208   R_0 cannot be pointed out. However, despite the uncertainty regarding v in this population, we

209   estimated a distribution of R_0 consistent with previous estimates. While the mode of distribution

210   for R_0 was 6.7, the validity of this value depends on the validity of our prior distribution of v,

211   which was not supported by any published evidence of this refugee population. Nevertheless,

212   Demographic and Health Survey data of the Rohingya population in Myanmar indicated a close

213   value from 40-50% as the coverage of DTP (Ministry of Health and Sports, 2017).

214   Ascertainment rates were jointly estimated only by using the epidemiological case data and the

215   population size.

216   What we have shown in the present study is that when we have an access to not only the

217   initial growth rate of the epidemic but also the incidence data around the time at which peak

218   incidence is observed, R_0 and susceptible fraction can potentially be jointly quantified. Even

219   without explicit estimate of the initially immune fraction, we have shown that an indication of

220   the possible value of R_0 can be obtained through uncertainty analysis. LHS appeared to be

221   particularly useful in the setting of refugee camp in which the background health status is not

222   well quantified (Helton & Davis, 2002; Nishiura et al., 2017). LHS can offer probabilistic

223   distribution of the outcome measure, R_0 in our case, and this method appeared to be particularly

224   useful when one or more uncertain input information exist (Elderd et al., 2006; Coelho et al.,

225   2008; Samsuzzoha et al., 2013; Gilbert et al., 2014). While Bayesian modeling has replaced LHS

226   to some extent of uncertainty analysis as it can also offer posterior distributions of even uncertain

227   parameters (Elderd et al., 2006; Coelho et al., 2008), there could be an issue of identifiability

228   when two or more parameters are evidently correlated, e.g. as anticipated between R_0 and v in

229   our model (4). In such an instance, we cannot be sure if the limited epidemic data with the

230   Bayesian estimation method can offer identifiable distributions for all parameters, and then LHS

231   can remain to act as a useful tool for uncertainty analysis.

232   Estimated small ascertainment rate during the epidemic is considered as reflecting the

233   time-dependent diagnostic practice at a local level. In fact, the small ascertainment rate can lead

234   us to observing the low case fatality risk of diphtheria in the Cox's Bazar that has been estimated

235   to be small (27/2526=1%), although the right censoring would of course matter for the real time

236   interpretation (Nishiura et al., 2009; Mizumoto et al., 2015). Nevertheless, cases could have died

237   in the community unnoticed with low specificity of the case definition, and this is endorsed as a

238   possible reason for observing the small number of deaths by the WHO (2017d). A follow-up

239   study in this regard should be conducted in the future.

240   Several limitations must be noted. First, our model rested on a homogeneous mixing

241   assumption. No heterogeneous patterns of transmission, including contact patterns and age-

242   dependency were taken into account due to shortage of information. In addition, the time-

243   dependent heterogeneity, including the reduced transmission potential due to contact tracing and

244   rapid hospitalization, was not explicitly taken into account due to insufficiency of the data. If

245   there were any additional indications or datasets that would allow explicit quantification of the

246   effective reproduction number from 12 December, that could give additional insights into the

247   success of control measures. Second, for similar reasons, no spatial information was explicitly

248   incorporated into the model. Third, a little more realistic features of refugee population, such as

249   the impact of migration on the epidemic were unfortunately discarded in the present study.

250   Similarly, one could investigate how overcrowding and malnutrition in the deprived population

251   would help enhance the spread of diphtheria, given sufficient data backup from epidemiological

252   investigations.

253   While these features need to be explicitly quantified in the future, we believe that our

254   study adds an important piece of evidence to the literature on diphtheria. The transmissibility of

255   diphtheria in the refugee population was estimated to be consistent with that in an endemic

256   setting and mass vaccination must satisfy at least the coverage of 86% to halt the major epidemic

257   of diphtheria.

Conclusions

The present study estimated R_0 of diphtheria in the Rohingya refugee camp, explicitly accounting for case ascertainment and previously immune fraction. Since previously immune fraction v of the refugee population was not precisely known, uncertainty analysis of R_0 was conducted with an input parameter assumption for v employing the Latin Hypercube sampling. R_0 ranged from 4.7 to 14.8 with the median estimate at 7.2. LHS can offer probabilistic distribution of the outcome measure, and this method appeared to be particularly useful in the setting of refugee camp in which the background health status is poorly quantified.

References

Anderson RM, May RM. 1982. Directly transmitted infectious diseases: Control by vaccination. Science 215(4536): 1053-1060.

Asai Y, Nishiura H. 2017. Joint estimation of the transmissibility and severity of Ebola virus disease in real time. Journal of Biological Systems 25(4): 587-603.

Banerji A, Ahmed R. 2017. Rohingya 'rather die' than return to oppression in Myanmar. Digital Journal, 15 December 2017. Available from: http://www.digitaljournal.com/news/world/rohingya-rather-die-than-return-to-oppression-in-myanmar/article/510061#ixzz52RF2vNh9

Coelho FC, Codeço CT, Struchiner CJ. 2008. Complete treatment of uncertainties in a model for dengue R0 estimation. Cad Saude Publica. 24(4):853-61.

Dinh L, Chowell G, Mizumoto K, Nishiura H. 2016. Estimating the subcritical transmissibility of the Zika outbreak in the State of Florida, USA, 2016. Theor Biol Med Model. 13(1):20.

280   Elderd BD, Dukic VM, Dwyer G. 2006. Uncertainty in predictions of disease spread and
281   public health responses to bioterrorism and emerging diseases. Proc Natl Acad Sci U S A.
282   103(42):15693-7.

283   Ejima K, Nishiura H. 2018. Real-time quantification of the next generation matrix and age-
284   dependent forecasting of pandemic influenza H1N1 2009 in Japan. Annals of
285   Epidemiology 2018; in press (10.1016/j.annepidem.2018.02.010).

286   Endo A, Nishiura H. 2015. Transmission dynamics of vivax malaria in the republic of Korea:
287   Effectiveness of anti-malarial mass chemoprophylaxis. Journal of Theoretical Biology
288   380:499-505.

289   Gilbert JA, Meyers LA, Galvani AP, Townsend JP. 2014. Probabilistic uncertainty analysis
290   of epidemiological modeling to guide public health intervention policy. Epidemics 6:37-
291   45.

292   Guzek J, Siddiqui R, White K, van Leeuwen C, Onus R. 2017. Health survey in Kutupalong
293   and Balukhali refugee settlements, Cox's Bazar, Bangladesh. Medecins Sans Frontieres:
294   Belgium, 2017. Available from:
295   https://www.msf.org/sites/msf.org/files/coxsbazar_healthsurveyreport_dec2017_final1.pd
296   f

297   Helton JC, Davis FJ. 2002. Illustration of sampling-based methods for uncertainty and
298   sensitivity analysis. Risk Anal. 22(3):591-622.

299   Hosseinpoor AR, Bergen N, Schlotheuber A, Gacic-Dobo M, Hansen PM, Senouci K,
300   Boerma T, Barros AJ. 2016. State of inequality in diphtheria-tetanus-pertussis
301   immunisation coverage in low-income and middle-income countries: a multicountry
302   study of household health surveys. Lancet Glob Health 4(9):e617-26.

303   Klinkenberg D, Nishiura H. 2011. The correlation between infectivity and incubation period

304   of measles, estimated from households with two cases. J Theor Biol 284: 52–60.

305   Kolibo DV, Romaniuk SI. 2001. Mathematical model of the infection process in diphtheria

306   for determining the therapeutic dose of antitoxic anti-diphtheria serum]. Ukr Biokhim Zh

307   73(2):144-51 (in Russian).

308   Ministry of Health and Sports, Myanmar. 2017. Myanmar Demographic and Health Survey

309   2015-16. Nay Pyi Taw, Myanmar & The DHS Program, ICF, USA. 2017. Available

310   from: https://dhsprogram.com/pubs/pdf/FR324/FR324.pdf

311   Mizumoto K, Saitoh M, Chowell G, Miyamatsu Y, Nishiura H. 2015. Estimating the risk of

312   Middle East respiratory syndrome (MERS) death during the course of the outbreak in the

313   Republic of Korea, 2015. International Journal of Infectious Diseases 39:7-9. doi:

314   10.1016/j.ijid.2015.08.005.

315   Nishiura H, Klinkenberg D, Roberts M, Heesterbeek JA. 2009. Early epidemiological

316   assessment of the virulence of emerging infectious diseases: a case study of an influenza

317   pandemic. PLoS One 4(8):e6852. doi: 10.1371/journal.pone.0006852.

318   Nishiura H. 2010. Correcting the actual reproduction number: A simple method to estimate

319   R0 from early epidemic growth data. International Journal of Environmental Research

320   and Public Health 7(1): 291-302.

321   Nishiura H, Chowell G, Safan M, Castillo-Chavez C. 2010. Pros and cons of estimating the

322   reproduction number from early epidemic growth rate of influenza A (H1N1) 2009.

323   Theoretical Biology and Medical Modelling 7: 1

324   Nishiura H, Kinoshita R, Mizumoto K, Yasuda Y, Nah K. 2016. Transmission potential of
325   Zika virus infection in the South Pacific. International Journal of Infectious Diseases.
326   45:95-7.
327   Nishiura H, Tsuzuki S, Yuan B, Yamaguchi T, Asai Y. 2017. Transmission dynamics of
328   cholera in Yemen, 2017: a real time forecasting. Theor Biol Med Model 14:14.
329   Rusmil K, Gunardi H, Fadlyana E, Soedjatmiko, Dhamayanti M, Sekartini R, Satari HI,
330   Risan NA, Prasetio D, Tarigan R, Garheni R, Milanti M, Hadinegoro SR, Tanuwidjaja S,
331   Bachtiar NS, Sari RM. 2015. The immunogenicity, safety, and consistency of an
332   Indonesia combined DTP-HB-Hib vaccine in expanded program on immunization
333   schedule. BMC Pediatr 15:219.
334   Samsuzzoha M, Singh M, Lucy D. 2013. Uncertainty and sensitivity analysis of the basic
335   reproduction number of a vaccinated epidemic model of influenza. Appl Math Model.
336   37(3):903–915.
337   Sanchez MA, Blower SM. 1997. Uncertainty and sensitivity analysis of the basic
338   reproductive rate, tuberculosis as an example. Am J Epidemiol. 145(12):1127–1137.
339   Sangal L, Joshi S, Anandan S, Balaji V, Johnson J, Satapathy A, Haldar P, Rayru R,
340   Ramamurthy S, Raghavan A, Bhatnagar P. 2017. Resurgence of Diphtheria in North
341   Kerala, India, 2016: Laboratory Supported Case-Based Surveillance Outcomes. Front
342   Public Health 5:218.
343   Sornbundit K, Triampo W, Modchang C. 2017. Mathematical modeling of diphtheria
344   transmission in Thailand. Comput Biol Med 87:162-168.
345   Stocks P. 1930. Infectiousness and immunity in regard to chickenpox, whooping-cough,
346   diphtheria, scarlet fever and measles. Proc R Soc Med 23:1349-68.

347   Torrea M, Ortega D, Torera JL. 2017. A modeling of a Diphtheria epidemic in the refugees

348   camps. bioRxiv Posted October 27, 2017. doi: https://doi.org/10.1101/208835

349   Tsuzuki S, Lee H, Miura F, Chan YH, Jung S, Akhmetzhanov AR, Nishiura H. 2017.

350   Dynamics of the pneumonic plague epidemic in Madagascar, August to October 2017.

351   Eurosurveillance 22(46):pii=17-00710.

352   World Health Organization (WHO). 2017a. Diphtheria Outbreak Response Update: Cox's

353   Bazar, Bangladesh – Update #2 (27 December 2017). World Health Organization:

354   Geneva, 2017. Available from:

355   https://reliefweb.int/sites/reliefweb.int/files/resources/bancxbdiphtheriaresponseupdate22

356   71217.pdf

357   World Health Organization (WHO). 2017b. Early Waning, Alert and Response System

358   (EWARS). WHO: Geneva, 2017. Available from:

359   http://www.who.int/emergencies/kits/ewars/en/

360   World Health Organization (WHO). 2017c. Minutes of Health Sector Meeting, 27 December

361   2017. WHO: Bangladesh, 2017. Available from:

362   https://www.humanitarianresponse.info/system/files/documents/files/minutes_of_health_

363   sector_meeting_27_december_2017.pdf

364   World Health Organization (WHO). 2017d. Mortality and Morbidity Weekly Bulletin. Cox's

365   Bazar, Bangladesh, Volume No 9: Week 49, 2017. WHO: Bangladesh, 2017. Available

366   from: http://www.searo.who.int/bangladesh/mmwbwk49171224.pdf?ua=1

367   World Health Organization (WHO). 2018. Weekly Situation Report #9. WHO: Bangladesh,

368   2018. Available from: https://reliefweb.int/sites/reliefweb.int/files/resources/sitrep09.pdf

369

Figures

370 **Figures**

371 **Figure 1. Daily incidence of diphtheria cases in Rohingya refugee camp, 2017**

372 Daily number of new cases as extracted from the latest open data (WHO, 2017a). The vertical

373 axis represents the total of confirmed, probable and suspected cases. By 11 December 2017, the

374 count represents suspected cases. On and after 12 December 2017, the case definition was

375 improved, and probable cases replaced the majority.

376 **Figure 2. Estimated values of the basic reproduction number and case ascertainment**

377 **rate**

378 Univariate probability distribution of the basic reproduction number, a_1 by 11 December and a_2

379 from 12 December from Latin Hypercube sampling ($n = 1,000$). During the Latin Hypercube

380 sampling, the vaccination coverage, v, has a symmetric triangular distribution ranging from 0.0

381 to 0.7.

382 **Figure 3. Estimated correlations in each pair of estimated parameters, and comparison**

383 **between observed and predicted epidemic curves**

384 Three panels except for right lower panel represent two-dimensional plot of estimated

385 parameters. During the Latin Hypercube sampling ($n = 1,000$), the vaccination coverage, v, has a

386 symmetric triangular distribution ranging from 0.0 to 0.7. Lower right panel is the comparison

387 between observed and predicted epidemic curves. Bars constituting the epidemic curve show the

388 observed data, while dots indicate predicted epidemic curve from Latin Hypercube sampling ($n =$

389 1,000).

390   **Figure 4. Sensitivity of R_0 with respect to the serial interval**

391   R_0 was estimated with variable values of the coefficient of variations (CV) of the serial interval.

392   Mean serial interval was fixed at 8 days. Variations of R_0 along the vertical axis reflects the

393   uncertainty associated with the initially immune fraction v of the Rohingya refugee population.

394

Figure 1

Daily incidence of diphtheria cases in Rohingya refugee camp, 2017

Daily number of new cases as extracted from the latest open data (WHO, 2017a). The vertical axis represents the total of confirmed, probable and suspected cases. By 11 December 2017, the count represents suspected cases. On and after 12 December 2017, the case definition was improved, and probable cases replaced the majority.
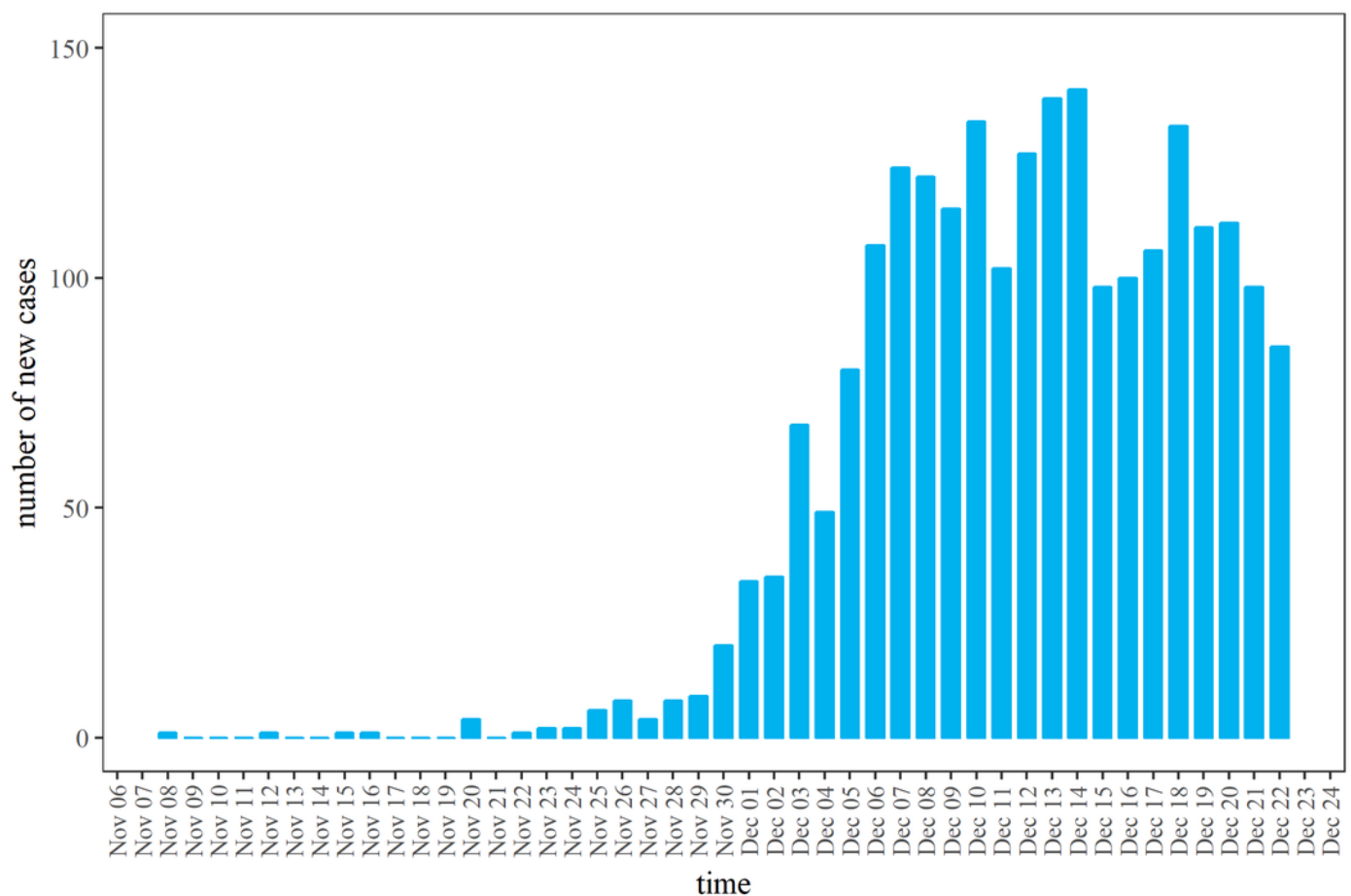
Figure 2

Estimated values of the basic reproduction number and case ascertainment rate

Univariate probability distribution of the basic reproduction number, a_1 by 11 December and a_2 from 12 December from Latin Hypercube sampling ($n = 1,000$). During the Latin Hypercube sampling, the vaccination coverage, v, has a symmetric triangular distribution ranging from 0.0 to 0.7.
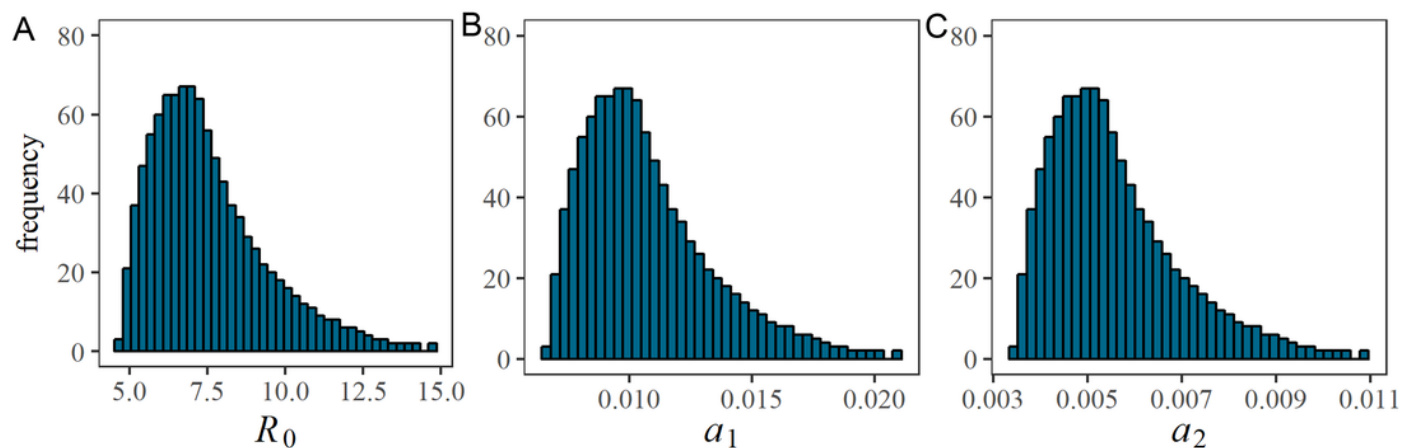
Figure 3

Estimated correlations in each pair of estimated parameters, and comparison between observed and predicted epidemic curves

Three panels except for right lower panel represent two-dimensional plot of estimated parameters. During the Latin Hypercube sampling ($n = 1,000$), the vaccination coverage, v, has a symmetric triangular distribution ranging from 0.0 to 0.7. Lower right panel is the comparison between observed and predicted epidemic curves. Bars constituting the epidemic curve show the observed data, while dots indicate predicted epidemic curve from Latin Hypercube sampling ($n = 1,000$).
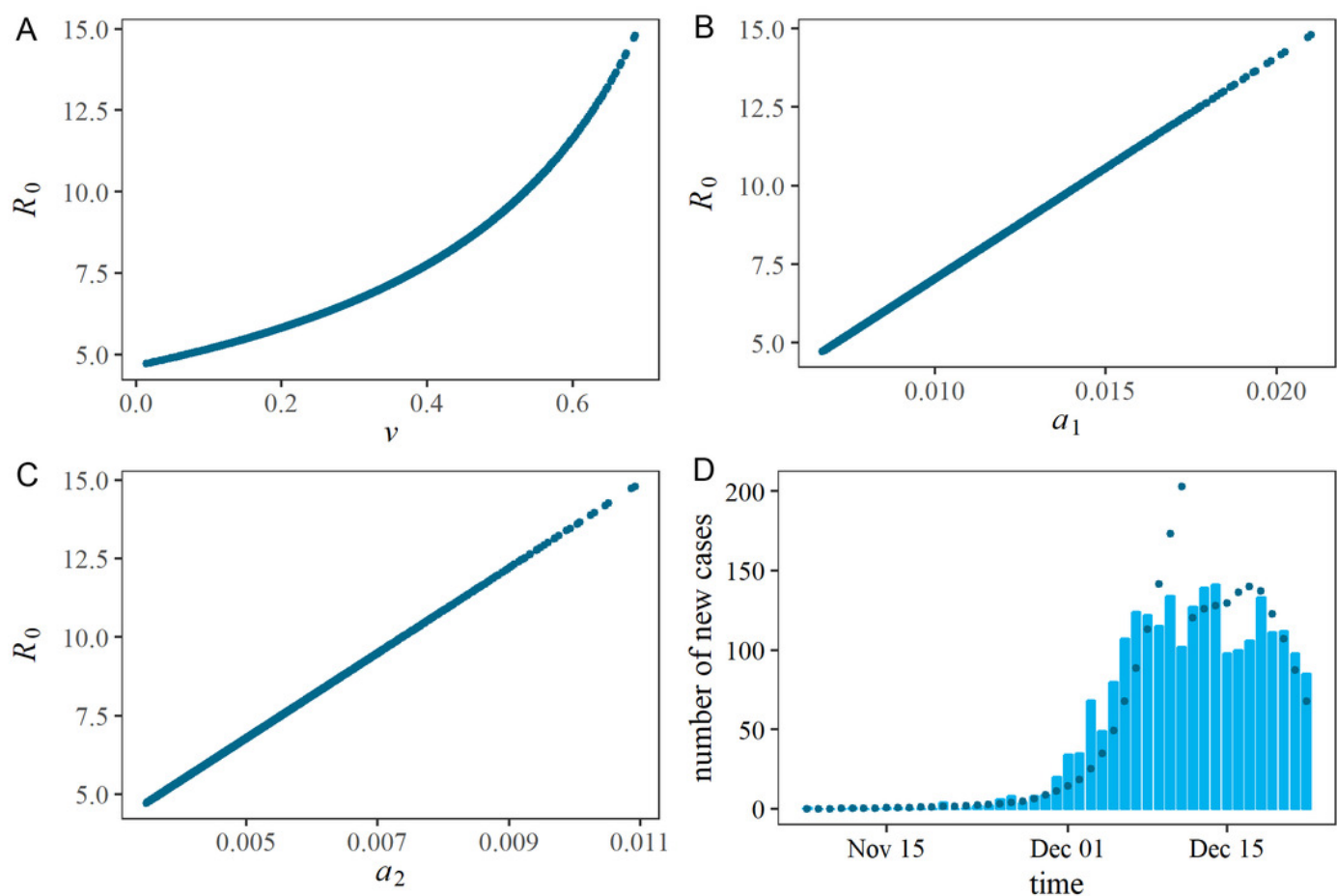
Figure 4

Sensitivity of R_0 with respect to the serial interval

R_0 was estimated with variable values of the coefficient of variations (CV) of the serial interval. Mean serial interval was fixed at 8 days. Variations of R_0 along the vertical axis reflects the uncertainty associated with the initially immune fraction v of the Rohingya refugee population.